Supplementary Information

Actin-driven Golgi apparatus dispersal during collective migration of epithelial cells

Khuntia *et al.*

This document contains:

SUPPLEMENTARY MATERIALS AND METHODS

Cell culture. All the experiments were done using the Madin-Darby canine kidney (MDCK) epithelial cell line and Caco-2 cells (ATCC-HTB-37) derived from colon tissue. Tetracyclineresistant Wild-type MDCK (MDCK-WT) cell lines were a gift from Yasuyuki Fujita. Cells were cultured in Dulbecco's modified Eagle's medium supplemented with GlutaMax (Gibco) with 10% fetal bovine serum (tetracycline-free FBS, Takara Bio) and 10 U mL^{-1} penicillin and 10 µg mL^{-1} streptomycin (Pen-Strep, Invitrogen) in an incubator maintained at 37°C and 5% CO2, unless mentioned otherwise. To establish a stable MDCK cell line constitutively over expressing Golgi localized mDsRedGolgi7, MDCK cells were transfected with the plasmid DNA using Lipofectamine 2000 (Invitrogen). Selection pressure was provided in form of medium (DMEM GlutaMAX) containing 400 µg mL^{-1} geneticin (Invitrogen). Clones were picked using cloning cylinders following a visual fluorescence confirmation. Subsequently, maintenance and passaging of stable cell lines was done in medium containing 100 µg mL^{-1} geneticin. All transient plasmid DNA transfections were done using Lipofectamine 2000 (Invitrogen) following the manufacturer's protocol. Cells seeded in IBIDI culture inserts at 70% confluency were used for transfection of mutant proteins. Migration of the transfected cells was carried out 24-48 hours post transfection and samples were used for live cell imaging or fixed for immunostaining. In case of inducible MENA-EVH1 or trunc-GRASP65 plasmid, expression was induced with 5 µg mL^{-1} doxycycline in culture media 30 minutes prior to removal of culture inserts and migration was carried out in the induction medium. To carry out cell migration experiments as before (32), adhesive biocompatible silicone culture-insert (ibidi) was press-bonded to glass-bottom culture dish (ibidi). The two wells (dimensions: 3.25 mm × 7 mm; growth area per well 22 mm^2; cell free gap 0.5 mm) in the culture insert was seeded with 5×10^4 cells, suspended in 80 µL cell culture medium, and were allowed to adhere and form cell monolayer for 18 h at 37 °C in a 5% CO_2 humidified incubator. Following incubation period, the culture-insert was lifted off to initiate cell migration, and 2 mL media was added to the dish. For all migration experiments, 37 °C and in 5% CO_2 environment was maintained.

Caco-2 cells were cultured in Dulbecco's modified Eagle's medium supplemented with GlutaMax (Gibco) with 10% fetal bovine serum (tetracycline-free FBS, Takara Bio) and 10 U mL^1 penicillin and 10 µg mL^{-1} streptomycin (Pen-Strep, Invitrogen) in an incubator maintained at 37°C and 5% CO2. Caco-2 differentiation was carried out by culturing cells on glass-bottom plates supplied with cell culture medium containing 1% (NEAA) for 21 days. Wound healing experiments were carried out by creating scratch wounds in the differentiated Caco-2 monolayer. Wound healing was carried out for 4, 8 and 12 hours. To transiently transfect differentiated Caco2 cells, plasmid DNA transfection was adapted from a previous report (60). Briefly, plasmid DNA was prepared in Lipofectamine 3000 (Invitrogen, L3000001) and incubated for 40 minutes at room temperature (RT). To prepare the differentiated cells for transfection, the monolayer was rinsed twice with Opti Minimal Essential Medium (OptiMEM). Followed by two rinses with 0.25% trypsin and 2.2 mM EDTA respectively. The monolayer was rinsed with DMEM and finally with OptiMEM. Following this, the monolayer was submerged in 1 mL OptiMEM and 200 µL of plasmid DNA-Lipofectamine 3000 solution was added to the monolayer. Cells were incubated with the transfection solution for 4 hours at 37 °C. After 4 hours, the transfection solution was removed and rinsed with OptiMEM and the monolayer was fed with the differentiation medium

for 18-24 hours. To induce plasmid DNA expression in the transfected monolayer, cells were supplied with medium containing 5 μg mL^{-1} doxycycline 40 minutes before the start of cell migration.

Antibodies and plasmids. Source and dilution information for all primary and secondary antibodies used in immunofluorescence staining are given in Supplementary Table 1. Details of plasmids used in this study is listed in Supplementary Table 2.

Immunofluorescence. Cell fixation was done with 4% formaldehyde diluted in 1x phosphate buffered saline (PBS, pH 7.4) at RT for 10 minutes, followed by 1X PBS washes (three times). Cell permeabilization was carried out with 0.25% (v/v) Triton X-100 (Sigma) in PBS for 10 min at RT followed by washing thrice with PBS to remove the reagent. To block non-specific antibody binding samples were incubated in 2% BSA in PBST (0.1% v/v Triton X-100 in 1X PBS) at RT for 45 minutes. The blocking buffer was removed after 45 minutes, and the primary antibody dilution prepared in blocking buffer was added to the samples for 60 minutes at RT or at 4°C overnight. Afterward, samples were washed twice with PBST and thrice with 1X PBS. Next, secondary antibody tagged with AF 488/594 were (same dilution as primary) prepared in blocking buffer and added to the sample for 60 minutes at RT. To counterstain cell nuclei and F-Actin, the samples were added with a DNA-binding dye 4′,6-diamidino-2-phenylindole (DAPI, 1 μg mL^{-1} in PBS, Invitrogen) and phalloidin conjugated Alexa Fluor dye (Invitrogen) along with the secondary antibody solution. Lastly, a thorough washing of the samples was done with PBST and PBS before imaging.

SiR-actin staining. Actin fibers were stained with SiR-actin (SPIROCHROME, CY-SC001) as described by the manufacturer. Briefly, to prepare 1mM stock, the content of the vial was dissolved in 50 μL of anhydrous DMSO. A 50 nM staining solution was prepared in the culture medium and cells were incubated with the solution for 12-16 hours.

Cell-pulling experiments. A custom cell-pulling device was used to apply mechanical strain to an elastomeric membrane made of PDMS (SYLGARD 184, Corning), which served as the cell culture substrate. The set-up consisted of two brushless servo motors (FAULHABER), which enabled us to stretch the membrane uni- or bidirectionally through a mechanical construction of eccentric tappets and conrods. The PDMS chamber, containing a 20 mm × 20 mm membrane for cell culture, was made by casting PDMS in a Plexiglas mould at an elastomer to crosslinker ratio of 10:1. The PDMS was cured for 4 h at 70 °C. The chamber was then peeled off. Cells were then seeded on the collagen-coated membrane and grown overnight to achieve confluency. Next day, cell-pulling experiments were carried out by stretching the membrane unidirectionally with an impulse strain (25% s^{-1}). Cells were kept in the pulled condition for 15 min, 1 hours, 3 hours and 4 hours before fixation with 4% paraformaldehyde. Following fixing, the chamber was released from the cell-pulling device, and immunostained with GRASP65 antibody. Finally, the membrane was cut out of the PDMS chamber, and put onto a confocal coverslip (cells facing the coverslip) and imaged using confocal microscopy.

Calcium switch experiments. To block E-cadherin mediated AJs, confluent cell monolayers grown in culture inserts were first washed twice with calcium–magnesium free HEPES and then incubated with 4 mM EGTA (Sigma) in HEPES buffer (Invitrogen, pH 7.4) for 30 min at 37°C in a 5% CO_2 humidified incubator. Following the incubation periods, the calcium free medium was replaced with the cell culture medium with or without E-cadherin blocking monoclonal antibody DECMA-1 (Millipore, 10 µg mL^{-1}), and cells migration was carried out for 4 hours at 37°C in a 5% CO_2 humidified incubator.

Ultrastructure expansion microscopy. The ultrastructure expansion microscopy (U-ExM) for mDsRed Golgi MDCK cells was done as described previously (44), which was optimized to retain the mDsRed Golgi fluorescent protein during the expansion procedure. Briefly, mDsRed Golgi MDCK monolayer was allowed to migrate for 4 hours and fixed with U-ExM fixation solution (3% formaldehyde (Invitrogen) with 0.1% glutaraldehyde (Sigma) in 1X PBS). After, the samples were added with post-fix solution, which is prepared by adding 0.7% formaldehyde with 1% Acrylamide (Sigma) in 1X PBS, and kept for incubation 37℃ for 5 hr. Then, the sample immobilization was done in 100 µL of U-ExM monomer solution composed of 19% Sodium Acrylate (Sigma), 10% Acrylamide (Sigma), 0.1% N,N′-methylene bisacrylamide (Sigma) in 1X PBS supplemented with 0.5% ammonium persulfate (Sigma) initiator and tetramethyl ethylenediamine (Sigma) accelerator, on a strip of Parafilm and placed in a pre-cooled humid chamber. Gelation was allowed for 5 min on ice, followed by 37 °C in the dark for 1 hour. The sample denaturation was carried out by adding ~2 mL of denaturation buffer, prepared by adding 200 mM sodium dodecyl sulfate, 200 mM NaCl, and 50 mM Tris in ultrapure water, and the pH was to adjusted to 9. Further denaturation was carried out at 70 °C for 1 h. After denaturation, samples were incubated in deionized water twice for every 30 min and then overnight at RT. Expanded samples were then trimmed carefully to obtain all the stages of migration induced Golgi remodeling, mounted on 35mm glass bottom dishes (Ibidi) and imaged by confocal microscopy.

Confocal microscopy. Fluorescence images were acquired using 60X oil objective (PlanApo N 60x Oil, N.A=1.42, Olympus) mounted on an Olympus IX83 inverted microscope equipped with a scanning laser confocal head (Olympus FV3000). Time-lapse images of live samples were done in the live-cell chamber provided with the microscopy setup. 20 mM HEPES (Gibco) was used to maintain CO_2 levels.

Super-resolution microscopy. Images were acquired with a 60X oil objective (UPLSAPO60XS2, N.A=1.45, Olympus) mounted on an Olympus IX83 inverted microscope supplied with Yokogawa CSU-W1 (SoRa Disk) scanner.

Inhibition studies. Nocodazole (Sigma), a microtubule disrupting agent, was used to study role of microtubule dynamics. Jasplakinolide (Invitrogen), actin filament stabilizer and Cytochalasin D (Sigma), actin depolymerizer, were used to study role of actin dynamics in MIGAR. All the drugs were dissolved in DMSO to prepare the primary stock solution. Cell migration was carried out in presence of 2.5 µM Nocodazole for 30 minutes. Similarly, to induce and stabilize actin polymerization, cell migration was done in presence of 500 nM Jasplakinolide for 45 minutes, and to disrupt actin filaments, cell migration was carried out in presence of 500 nM Cytochalasin D.

Media containing the drug was added to the sample at different stages (0, 0.5, 2, and 4 hr) of migration, and the media was replaced with fresh media and migration was carried out till 4 hours (for the 4-hour time point, cells were fixed at 4.5 hour of migration). CK-666, cell-permeable inhibitor of actin assembly mediated by actin-related protein Arp2/3 complex, was obtained from Sigma. The powdered chemical form was dissolved in DMSO to make the stock. For fixed samples, MDCK monolayer migration was carried out in presence of 40 μM for 4 hours. For live cell imaging, 100 μM of CK-666 was used for 30 minutes. For differentiated Caco-2 cells, actin perturbation was carried out with Jasplakinolide (1 μM) Cytochalasin D (1 μM) for 4 hours and, CK-666 (500 μM). All the drugs were supplied in the differentiation medium.

Dispersion index measurement. To calculate dispersion index, first Golgi channel images were segmented to find Golgi objects using 3D iterative thresholding in 3D Suite-FIJI. Centroid values of the objects were extracted. Then, all the Golgi objects were merged to calculate the center of mass of Golgi. The distance between center of mass and centroid of Golgi objects were measured, and root mean square (RMS) value was calculated. RMS values were then divided by nuclear radius deduced from nuclear area measured after DAPI-based segmentation of nucleus. Centroid coordinates were used for XY scatter plots.

Image analysis. To analyze the distribution of the three different stages of Golgi organization, a 500X500 μm FOV of a migrating monolayer (2hr, 4hr, and 6hr) was divided in to 100 um width windows from the migrating edge. Golgi distribution was manually counted in each window and a bar graph was plotted. To show the Golgi distribution pattern in 2hr, 4hr, and 6hr migrating samples, F-Actin images were used to generate cell boundaries using ImageJ threshold tool. The cell boundaries thus generated were manually filled with a specific colour to show apical or equatorial dispersion or polarized Golgi distribution. To measure the distance between Golgi and nuclear centroid, time lapse images of mDsRed Golgi cells stained with Hoechst (CST) were used. Golgi and nuclei objects were segmented using the 3D Spot segmentation and 3D Nuclei Segmentation (beta), respectively, in ImageJ 3D Suite plugin. To monitor the diffusion of photoconverted Dendra2-ManII, images were taken in 488 and 561 channel at 1-minute interval for 30 minutes. Three ROIs were selected in the FOV and the median 561 nm signal intensity in each ROI in was calculated. The intensity values were plotted into a line-scatter plot. Change in the number of actin projections and rings were calculated by manually counting the actin projections and rings in each frame (40 frames), taken at 5-minute intervals for 30 minutes. To quantify the length and number of actin fibers, the SiR-actin stained images of actin were segmented using 3D iterative thresholding in 3D Suite-FIJI. The segmented objects were analyzed to get the length and number of actin fibers. Similarly, to compare the migration parameters (speed, tracks, theta change at each step and net displacement) of cells, cells were tracked through a timelapse series (10-12 hours) using the Manual Tracking plugin in FIJI. To calculate the distance between Golgi and centrosome, the YZ plane images was used and Golgi and Centrosome objects were identified manually by using Freehand Selection tool from ImageJ. The centroid value was extracted for each object and the distance between the Golgi and Centrosome centroid was represented as a Box and Whiskers plot. To quantify percentage of cells with the three types of Golgi organization, we have used δ–based measurements to manually categorize organization of

Golgi (apical, equatorial, and polarized) and counted for approximately 80-100 cells for control, drug treated and mutant constructs.

Statistical analysis. All statistical analysis was carried out in SigmaPlot 10.0. We found a specific distribution of the percentage of cells with the three types of Golgi organization during migration (**Figure 1c**, 4hr). To understand how the distribution pattern varied upon drug treatment or mutant expression, Chi square (χ^2) analysis was used. Under this analysis, the null hypothesis assumes that the observed frequencies for a categorical variable (Golgi organization) are identical to the expected frequencies for the same categorical variable. The control distribution of Golgi organization (apical, equatorial, and polarized) served as the expected frequency, and the drug treated or mutant-expression distribution was used as the observed frequency. The Chi square analysis was used to compare the effect of Jasplakinolide (**Supplementary figure 5c**), Cytochalasin D (**Supplementary figure 5c**), and CK666 treatment (**Figure 4h**). A similar analysis was also done to study the effects of expression of mutant constructs, AKAP450 (**Figure 3c**), MYO18A-PDZ, MENAΔGAB, MENAΔFAB, MENA-EVH1 and trunc-GRASP65 (**Figure 5i**).
Sample size (n) was maintained at 80-100 cells for control, drug-treated and mutant constructs. Unpaired t-test with Welch's correction was used for comparing two independent sample groups such as the change in number of actin projections per frame (**Figure 4f**, n=30 frames), change length and number of actin fibers (**Supplementary figure 7a**, n=7 cells), change in direction at each turn, net displacement (**Figure 6h** and **6i**, n= 10 cells) and, Golgi-centrosome distance (**Supplementary figure 9b**, n=12 cells). Scatter-bar plots were displayed as mean ± S.E.M. In Box-and-whiskers plot, center line denotes median, box displays the interquartile range, whiskers indicate range not including outliers (1.5x interquartile range). P-values greater than 0.05 were considered to be statistically not significant. No statistical methods were used to set sample size.
Quantification was done using data from at least three independent biological replicates.

Supplementary Table 1. Antibodies used in the work

Antibodies/Fluorophore	Catalog No.	Manufacturer	Dilution/Working concentration
DAPI (4′,6-diamidino-2-phenylindole)	D1306	Invitrogen	1 μg ml^{-1}
Alexa-Fluor-647 Phalloidin	8940	CST	1:40
Alexa-Fluor-555 Phalloidin	8953S	CST	1:40
Golgin-97(D8p2k)	13192S	CST	1:200
Gm130 (D6b1) Xp(R)	12480T,	CST	1:200
GRASP65	MA5-25148	Thermo	1:200
ZO-1	8193T	CST	1:200
MENA clone A351F7D9	MAB2635	Millipore	1:200
alpha-Tubulin (DM1A) Mouse mAb	3873S	CST	1:400
Anti-E-Cadherin, DECMA-1	MABT26	MERK	10 μg ml−1
anti-FLAG-M2 (monoclonal)	F1804	Sigma	1:500
MYO18A polyclonal antibody	PA5-76549	Thermo	1:200
GOLPH3 polyclonal antibody	PA5-100010	Thermo	1:200
Alexa Fluor Plus 594 donkey anti-mouse IgG secondary antibody	A32744	Invitrogen	Same as per primary antibody dilution
AlexaFluor 488, Goat anti-Mouse IgG (H+L) Cross-Adsorbed Secondary Antibody	A-11001	Invitrogen	Same as per primary antibody dilution
Alexa Fluor 488, Goat anti-Rabbit IgG (H+L) Cross-Adsorbed Secondary Antibody	A-11008	Invitrogen	Same as per primary antibody dilution
Anti-rabbit IgG (H+L), F(ab')2 Fragment (Alexa Fluor®555 Conjugate)	4413S	CST	Same as per primary antibody dilution

Anti-rabbit IgG (H+L), F(ab')2 Fragment (Alexa Fluor-647 Conjugate)	4414S	CST	Same as per primary antibody dilution

Supplementary Table 2. Plasmids used in the work

Plasmid	Source	Identifier	Comment
mDsRed-Golgi-7	Addgene	55832	Golgi residing protein
BARS WT-YFP BARS (S147A)-YFP BARS (S147D)-YFP BARS (D355A)-YFP	Alberto Luini/Carmen Valente		BASRs phosphorylation mutants
EGFP-GRASP55-T222E/T225E/T249E EGFP GRASP55-T222A/T225A	Alberto Luini/Carmen Valente		GRASP55 phosphorylation mutants
Dendra2-MannII-N-10	Addgene	57730	Phoconvertible Mannosidase II
AKAP450, GFP-AK1 AKAP450, FLAG-AK1 AKAP450, FLAG-AK1B AKAP450, GFP-AK1-B	Rosa M. Rios		AKAP450 mutants: Unable to bind microtubule
pMSCV-EGFP-MENA pMSCV-EGFP-MENA-DeltaFAB pMSCV-EGFPMENADeltaGAB	Yanzhuang Wang		MENA mutant: Unable to bind actin
MYO18A-PDZ	This work (GENE SYNTHESIS)		MYO18A mutant: unable to bind actin
MENA-EVH1	This work (GENE SYNTHESIS)		MENA mutant: Golgi interacting domain

Supplementary Movie Legends

Supplementary Movie 1. Time lapse movie of mDsRed Golgi MDCK cells showing Golgi reorganization during migration. Images were taken at 30 minute interval for 4 hours.

Supplementary Movie 2. Time lapse movie of cell migration carried out in presence of DECMA1 showing absence of equatorial Golgi dispersion and single cell-like migration. Images were taken at 30 minute interval for 5 hours.

Supplementary Movie 3. Time lapse movie of Diffusion of Dendra2-ManII after photoconversion. Images were taken at 1 minute interval for 30 minutes.

Supplementary Movie 4. Time lapse movie of Golgi ribbon disentanglement following interaction with actin projections. Images were taken at 1 second interval for 1 minute.

Supplementary Movie 5. Time lapse movie of Golgi ribbon fragmentation carried out by actin ring. Images were taken at 1 second interval for 1 minute.

Supplementary Movie 6 and 7. Time lapse movie of formation of actin rings and projections, and interaction with Golgi observed in Utrophin GFP-mDsRed Golgi cells. Images were taken at 1 second interval for 1 minute.

Supplementary Figure Legends

Supplementary Figure 1. Characterization of equatorial Golgi dispersion in MDCK collective cell migration. A) Fluorescence images showing the Golgi organization after 0 hr of migration. The δ value for the selected cell (yellow arrow) shown at the bottom-left corner of the Golgin-97 image. Scale bar, 20 μm. **B)** Fluorescence images showing the Golgi organization after 2 hr of migration. Black dotted arrow shows the direction of migration. The δ value for the selected cell (yellow arrow) shown at the bottom-left corner of the Golgin-97 image. Scale bar, 20 μm. **C)** Fluorescence images showing the Golgi organization after 6 hr of migration. Black dotted arrow shows the direction of migration. The δ value for the selected cell (yellow arrow) shown at the bottom-left corner of the Golgin-97 image. Scale bar, 20 μm. **D)** Immunostained images of migrating monolayer showing Golgi localization with respect to apical-marker ZO-1. Yellow dotted boxes mark the cells showing 1: Apical, 2: Equatorial and 3: Polarized Golgi localization, in the YZ-view. The δ values for the selected cells (yellow box) shown at the bottom-left corner of the YZ-view panels. Scale bar 20 μm. **E)** Schematic describing the change in Golgi organization during migration. **F)** Immunostained images of mDsRed Golgi MDCK cell line showing uniform expression and localization of the fluorescence protein in all cells (inset, left). The image on right recapitulates equatorial Golgi dispersion in the mDsRed Golgi cell line. Black dotted arrow shows the direction of migration. The δ value for the selected cell (yellow arrow) shown at the bottom left corner in right panel. Scale bar, 5 μm. **G)** Schematics describing the measurement of dispersion index. d: distance between individual Golgi object centroid (black dots) and entire Golgi center of mass (red dot), N: number of Golgi objects, R: Nuclear radius. **H)** Scatter plot showing Golgi dispersion in XY plane with time of migration and corresponding dispersion index (δ) values for each timepoint. Dispersion index value gradually increases till 1.5 hr, and then shows a decline till 3.5 hours. **I)** A Line-scatter plot (top) showing change in δ values with time of migration for several cells. Corresponding Line-scatter plot (bottom), showing mean δ values for all the cells. δ value peaked at 1.5 hours. Error bars represent standard error in mean (±S.E.M). n=7 cells. **J)** A Line scatter plot of normalized migration speed (top) of cells showing an increase in speed after 3 hours. Corresponding Line-scatter plot (bottom) showing mean normalized speed for all the cells. Error bars represent ± S.E.M. n=7 cells.

Supplementary Figure 2. Establishment of Caco-2 epithelial model system and MIGAR in Caco-2 collective cell migration. A) Immunostained images of undifferentiated Caco-2 cells showing Golgi dispersed across the cytoplasm and irregular cell shape. Scale bar 20 μm. **B)** Immunofluorescence images of 21 days differentiated Caco-2 cells showing apically localized Golgi and regular cell shape. The δ value for the selected cell (yellow arrow) shown at the bottom left corner of the GM130 image. Scale bar 20 μm. **C)** Immunostained images of differentiated Caco-2 at 0 hr of migration showing apical Golgi. The δ value for the selected cell (yellow arrow) shown at the bottom-left corner of the Golgin-97 image. Scale bar 10 μm. **D)** Immunofluorescence images of Caco-2 cells after 4 hours of migration. Cells show polarized Golgi at the edge of monolayer (top), and equatorial Golgi dispersion in cells behind the migrating edge (bottom).

Black dotted arrow denotes the direction of migration. The δ values for the selected cells (yellow arrow) shown at the bottom-left corner of the Golgin-97 and GM130 image. Scale bar 10 μm. **E)** Immunofluorescence images of Caco-2 cells after 8 hours of migration showing equatorial Golgi organization. Black dotted arrow denotes the direction of migration. The δ value for the selected cell (yellow arrow) shown at the bottom-left corner of the GM130 image. Scale bar 10 μm.

Supplementary Figure 3. The migration induced Golgi remodeling is an active process and property of the collective cell migration. A) Schematic on left describes the experimental plan. Fluorescence images of the cell monolayer following cell-pulling, displays the apical Golgi localization in Control sample and loss of equatorially dispersed Golgi in all the stretched monolayers. The blue dotted arrow on top shows the uniaxial direction of stretching. Left to right, Control, 15 min, 1 hr, 3 hr, 4 hr. The δ values for the selected cells (yellow arrow) shown at the bottom-left corner of the Golgin-97 panel. Scale bar, 10 μm. **B)** Fluorescence images showing the altered Golgi organization observed in the calcium switch experiment. Both control and EGTA samples exhibit equatorial dispersion in migrating cells (inset). But, continued migration in presence of E-cadherin blocking DECMA1 antibody shows loss of the transition state (inset). The δ values for the selected cells (yellow arrow) shown at the bottom-left corner of the insets. Scale bar, 10 μm. **C)** A montage of time-lapse images of migration carried out in presence of DECMA1 showing absence of equatorial dispersion and single cell like migration. Images were taken at 30minute interval for 5 hours (**Supplementary Movie 2**). Image dimension 211.30 X 211.30 μm. **D)** Fluorescence images capturing equatorial Golgi dispersion using several Golgi markers, δ values included for Golgi dispersion with each marker at the bottom-left corner. Scale bar, Caco-2GM130: 5 μm, MDCK-GRASP65: 2.5 μm, MDCK-Dendra2-ManIIa: 5 μm, MDCK-Golgin-97: 5 μm, MDCK-mDsRed Golgi: 5 μm.

Supplementary Figure 4. Migration induced Golgi remodeling is independent of mitotic remodeling pathway. A) Expression of constitutively active and phosphorylation inactive GRASP55 mutants does not affect migration induced Golgi remodeling. The δ values for the selected cells (yellow arrow) shown at the bottom-left corner of the Golgin-97 panel. Scale bar 10 μm. **B)** Expression of the constitutively active and phosphorylation inactive mutants of BARS mutants does not hamper MIGAR. A single cell has been highlighted on the right from the yellow box area showing the equatorial dispersion. The δ values for the selected cells shown at the bottom left corner of the Golgin-97 image. Scale bar, 10 μm and 5 μm in the zoomed in panels.

Supplementary Figure 5. Role of actin dynamics in MIGAR. A) MDCK monolayer treated with Jasplakinolide (filament stabilization) and Cytochalasin D (filament depolymerization) displaying the effect on Golgi organization. Jasplakinolide treated cells (top panel) show lack of equatorial Golgi dispersion and formation of semi-circular actin aggresomes (Yellow asterisk). Cytochalasin D treated cells (bottom) also demonstrate absence of equatorial Golgi dispersion. Yellow dotted boxes are zoomed in on the right to show actin and Golgi organization in cells. Scale bar, 5 μm. **B)** Immunofluorescence images showing the migrating edge in control cells, and Jasplakinolide and Cytochalasin D treated cells. The δ values for the selected cells (yellow arrow) shown at the bottom-left corner of the Golgin-97 panel. Scale bar, 5 μm. **C)** Stacked column plots showing percentage of cells with the three types of Golgi organization in Jasplakinolide treated

cells (top), and Cytochalasin D treated cells (bottom). $p<0.001$, n=94 cells. **D)** A time-lapse montage of Utrophin GFP and mDsRed Golgi expressing cells showing actin cytoskeleton-Golgi interaction. Images were taken at 1 second interval for 1 minute. Yellow dotted box highlights one specific event of actin-Golgi interaction (**Supplementary Movie 6 and 7**). Image dimension: 4.45 X 4.45 µm. **E)** Time projected images of inhibition of formin mediated actin nucleation by SMIFH2 (left) and ML141 (right) in Utrophin GFP expressing cells do not show any change in actin ring and projection formation. Images were taken at 2 second interval for 1 minute. Image dimensions, SMIFH2: 15.02 X 15.02 µm, ML141: 20.64 X 20.64 µm. **F)** Fluorescence image showing the Golgi ribbon organization (inset) in control and CK-666 treated cells. Scale bar, 5 µm.

Supplementary Figure 6. Effect of actin perturbation on MIGAR in Caco-2 cells. Immunofluorescence images of control cells and cells treated with actin perturbing drugs. Left to right: Control, Jasplakinolide, Cytochalasin D, CK-666. Control cells show an organized Golgi, whereas drug treated cells show cytoplasmically dispersed Golgi with no specific organization. The δ value for the selected cell (yellow arrow) shown at the bottom-left corner of the Golgin-97 image, dispersion index not applicable to cells with cytoplasmically dispersed Golgi. The schematics on the bottom represents the difference in Golgi organization observed in control and drug treated cells. Scale bar 10 µm.

Supplementary Figure 7. Effect of MENA-EVH1 overexpression on front-rear actin organization. A) The Box and whisker plots display the comparisons of length of actin fibers (top) and number (bottom) of actin fibers in control cells and MENA-EVH1 expressing cells. n=7 cells. **B)** Immunofluorescence images showing localization of several actin markers, Arp3, pMLC and SiR-actin. The yellow dotted area marks the MENA-EVH1 construct expressing cells and the cyan dotted area marks the control cells. The images show no discernable change in actin front-rear organization between the control and MENA-EVH1 expressing cells. Scale bar 5 µm.

Supplementary Figure 8. Role of MENA-GRASP65 molecular pathway in MIGAR in Caco2 collective cell migration. A) Immunofluorescence images of Caco-2 collective cell migration after 12 hours, following doxycycline induction of MENA-EVH1 expression. Control cells (cyan dotted area) behind the migrating edge show equatorial Golgi whereas MENA-EVH1 expressing cell (yellow dotted area) show polarized Golgi. The δ values for the selected cells shown at the bottom-left corner of the GM130 image, in the respective color. Black dotted arrow denotes the direction of migration. Scale bar 10 µm. **B)** Immunofluorescence Caco-2 collective cell migration after 12 hours, following doxycycline induction of trunc-GRASP65 expression. Control cells (cyan dotted area) behind the migrating edge show equatorial Golgi compared to trunc-GRASP65 expressing cells (yellow dotted area) with polarized Golgi. The δ values for the selected cells shown at the bottom-left corner of the GM130 image, in the respective color. Black dotted arrow denotes the direction of migration. Scale bar 10 µm. **C)** A stacked column plot showing the reduction in percentage of cells with equatorial Golgi in Caco-2 cells expressing MENA-EVH1 construct. $p<0.001$, n=98 cells. **D)** A stacked column plot showing the reduction in percentage of cells with equatorial Golgi in Caco-2 cells expressing trunc-GRASP65 construct. $p<0.001$, n=98 cells.

Supplementary Figure 9. Loss of coherent intracellular polarization under conditions MENA-EVH1 overexpression. A) Immunostained image displaying the altered centrosome positioning with respect to Golgi. The YZ view shows the increased distance between Golgi and centrosome in MENA-EVH1 expressing cells. The yellow asterisk marks the centrosome position/signal. The δ value for the selected cell (yellow arrow) shown at the bottom-left corner of the XY-view image. Scale bar, 10 μm. **B)** A Box and whiskers plot representation highlighting the increased Golgi-centrosome distance under MENA EVH1 overexpression condition. $p<0.05$, n=12 cells.

Supplementary Figure 10. MIGAR is required for coherent intracellular polarization to allow persistent cell migration. A) The line scatter plots depict a comparison of Golgi position change and cell migration tracks in single cell migration (*Left*), and collective cell migration (*Right*). The black arrow denotes the direction of migration. **B)** Cell migration tracks for control MDCK cells (*Left*) and MDCK cells overexpressing MENA-EVH1 (*Middle*), and trunc-GRASP65 (*Right*). The black arrow denotes the direction of migration. Control cells exhibit long persistence directional migration whereas MENA-EVH1 and trunc-GRASP65 overexpressing cells show reduced persistent migration. The migration tracks of control cells (*Left*) orient with the direction of migration whereas the MENA-EVH1 and trunc-GRASP65 overexpressing cells appear random with respect to direction of migration. **C)** A box-and-whiskers plot of cell migration speed of control MDCK cells (boxes 1-10), MENA-EVH1 overexpressing cells (boxes 11-20), and trunc-GRASP65 overexpressing cells (boxes 21-30). Control cells and MENA-EVH1 overexpressing cells do no show any discernable difference, however, cells overexpressing trunc-GRASP65 construct show comparatively higher variation in migration speed. n = 10 frames. **D**) Schematic representing the measurement of change in angle during migration, θ in degrees. **E**) Scatter line plot of theta at each step in the migration trajectory of control MDCK cells showing small changes in direction during migration. **F**) Scatter line plot of theta at each step in the migration trajectory of MENA-EVH1 overexpressing MDCK cells showing large and variable changes in direction during migration. **G**) Scatter line plot of theta at each step in the migration trajectory of trunc-GRASP65 overexpressing MDCK cells showing large and variable changes in direction during migration. **H**) A box-and-whiskers plot showing significant difference in change in direction (θ) at each step for control MDCK cells and MDCK cells overexpressing MENA-EVH1 ($p < 0.001$) and trunc-GRASP65 ($p < 0.0001$). n = 10 cells. **I**) A box-and-whiskers plot of net displacement depicting a reduced displacement with expression of MENA-EVH1 ($p < 0.05$) and trunc-GRASP65 ($p < 0.0001$). n = 10 cells.

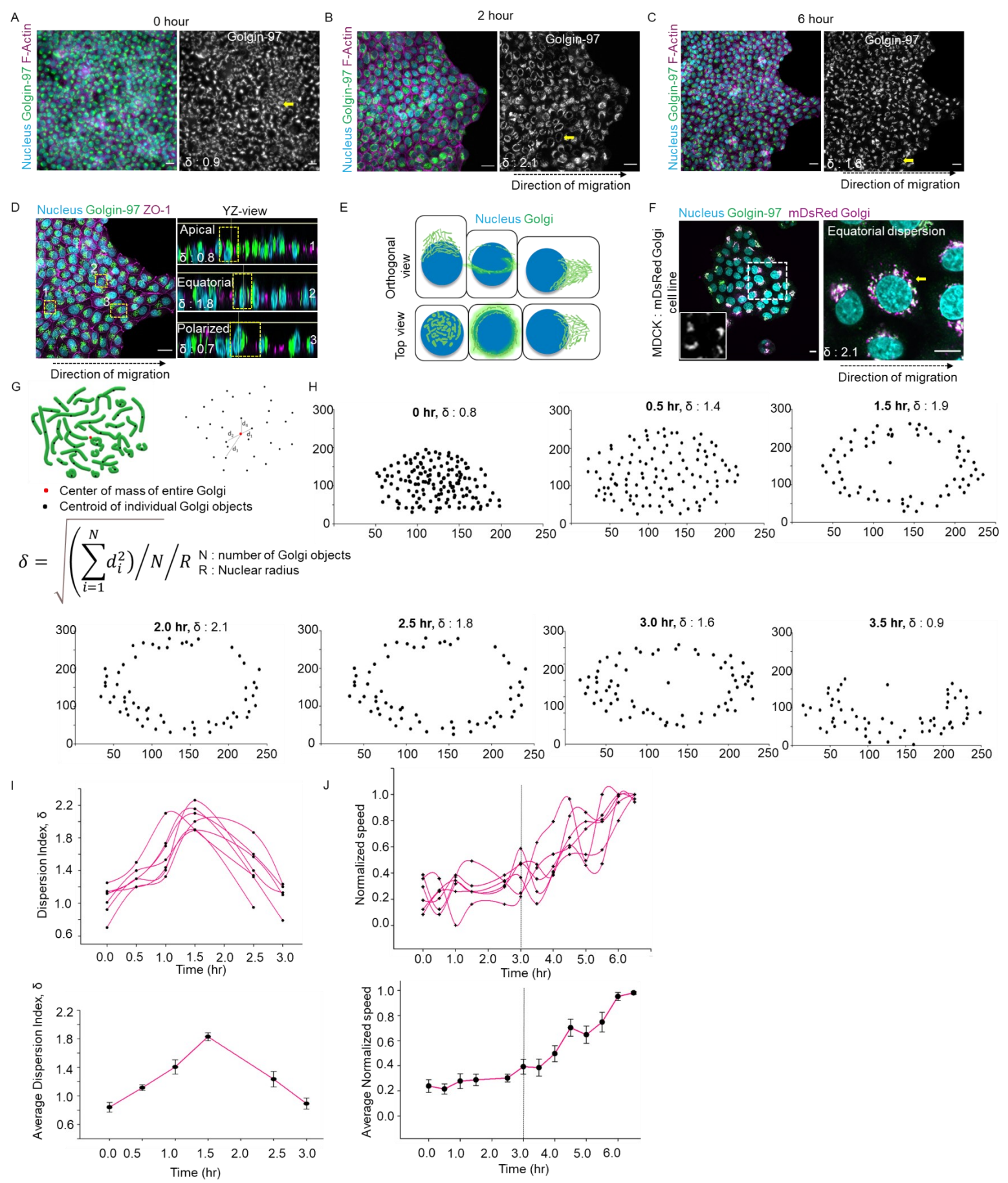

Supplementary Figure 1 : Characterization of equatorial Golgi dispersion in MDCK collective cell migration.

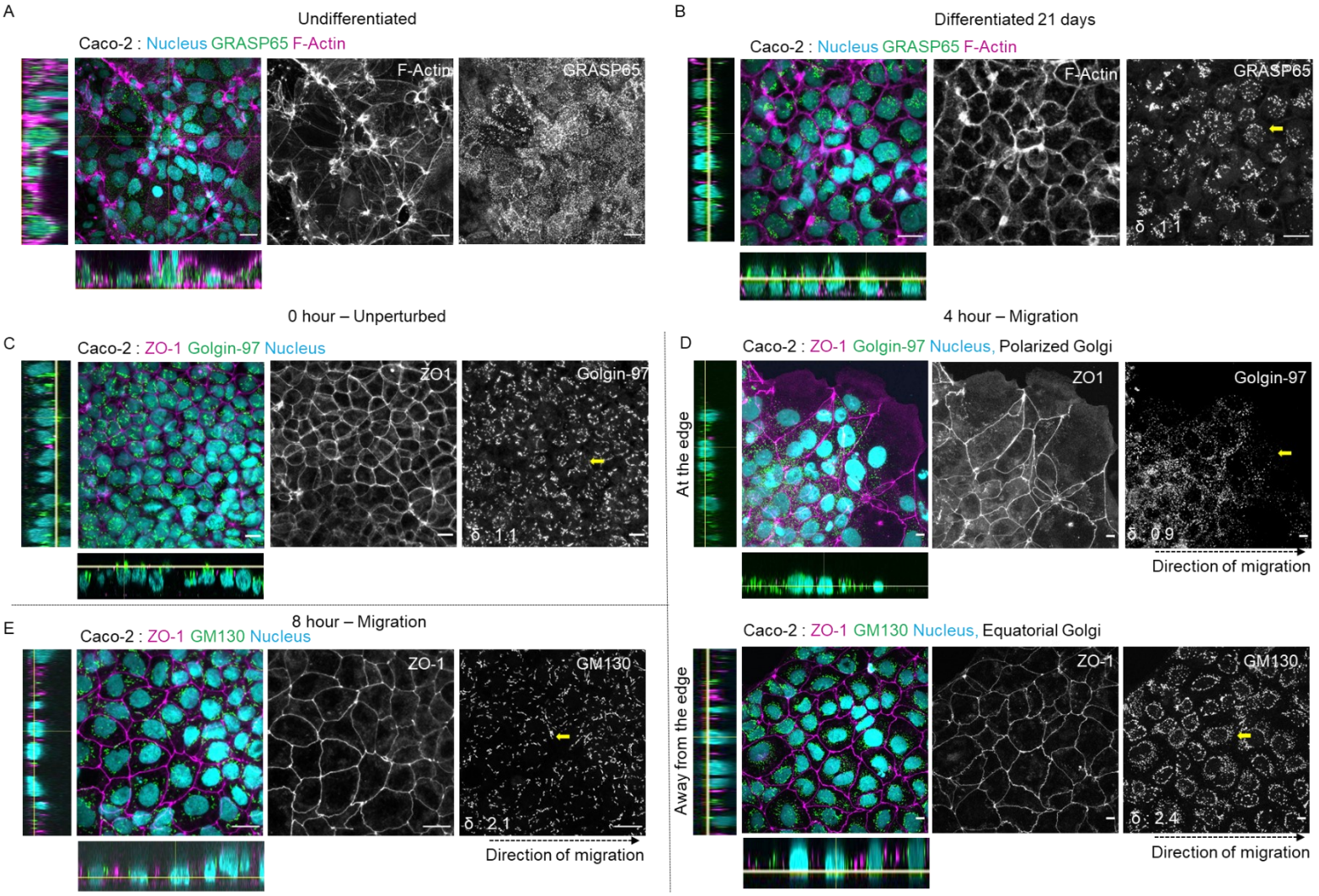

Supplementary Figure 2 : Establishment of Caco-2 epithelial model system and migration induced Golgi remodeling in Caco-2 collective cell migration.

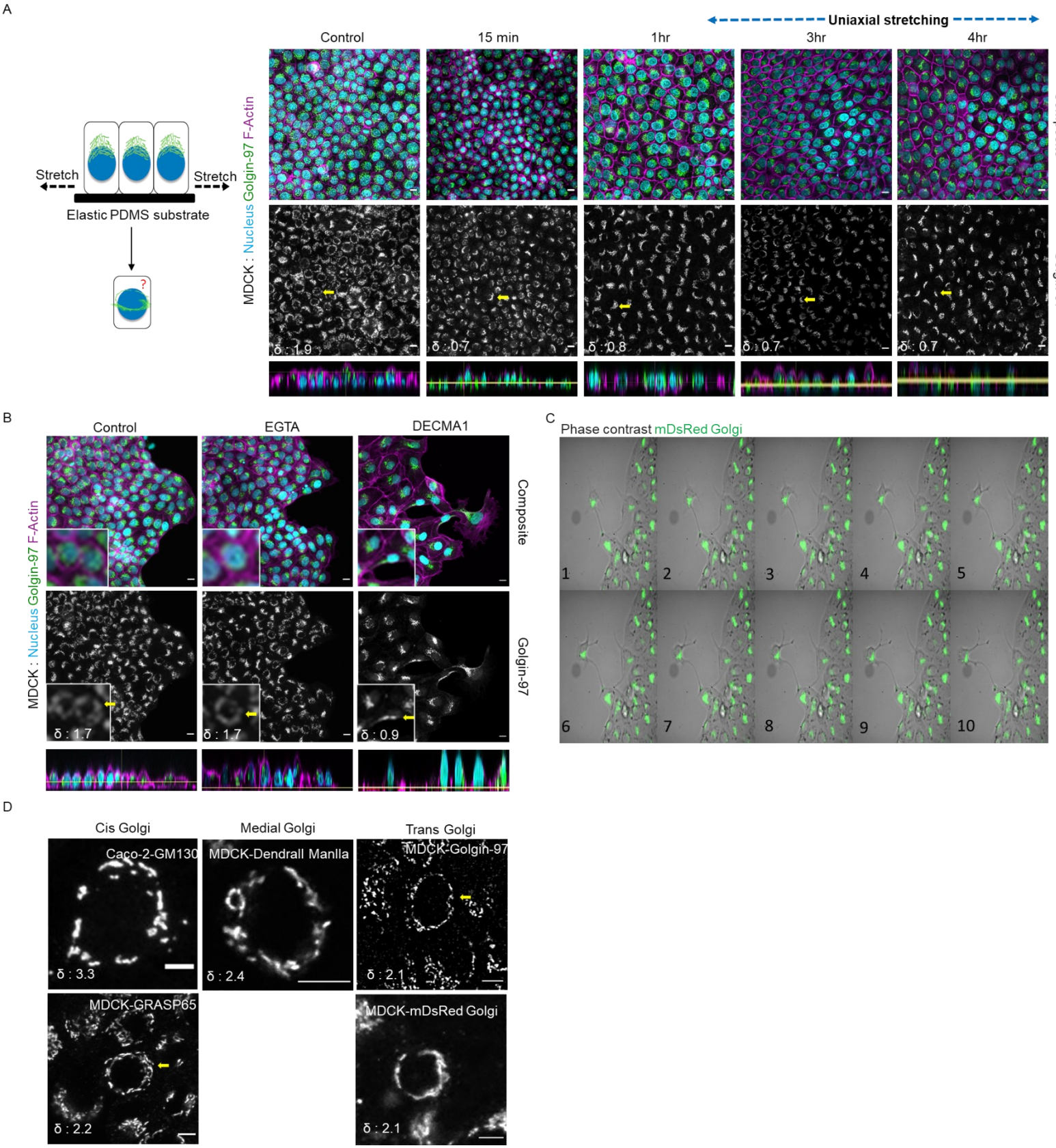

Supplementary Figure 3 : The migration induced Golgi remodeling is an active process and property of the collective cell migration.

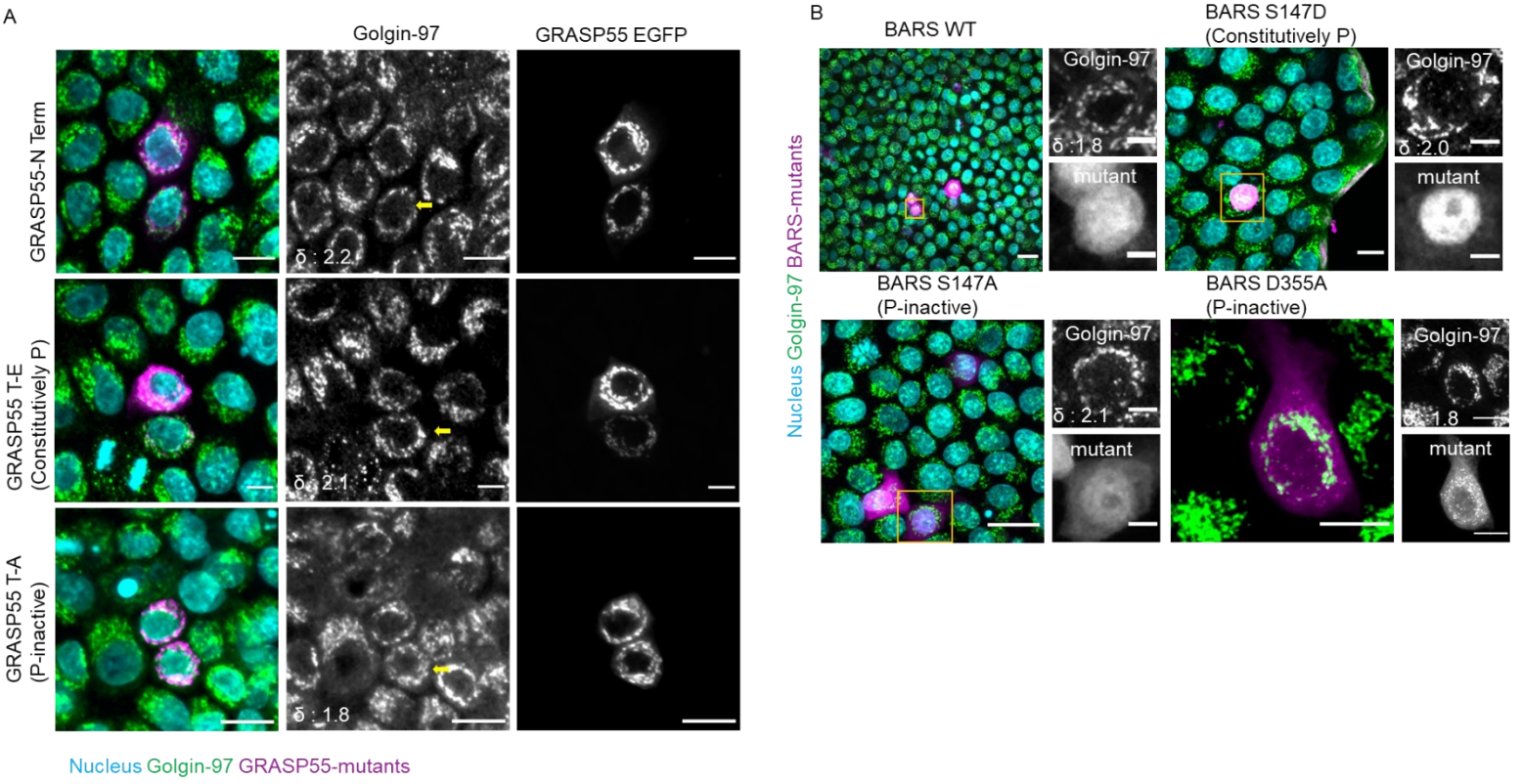

Supplementary Figure 4 : Migration induced Golgi remodeling is independent of mitotic remodeling pathway.

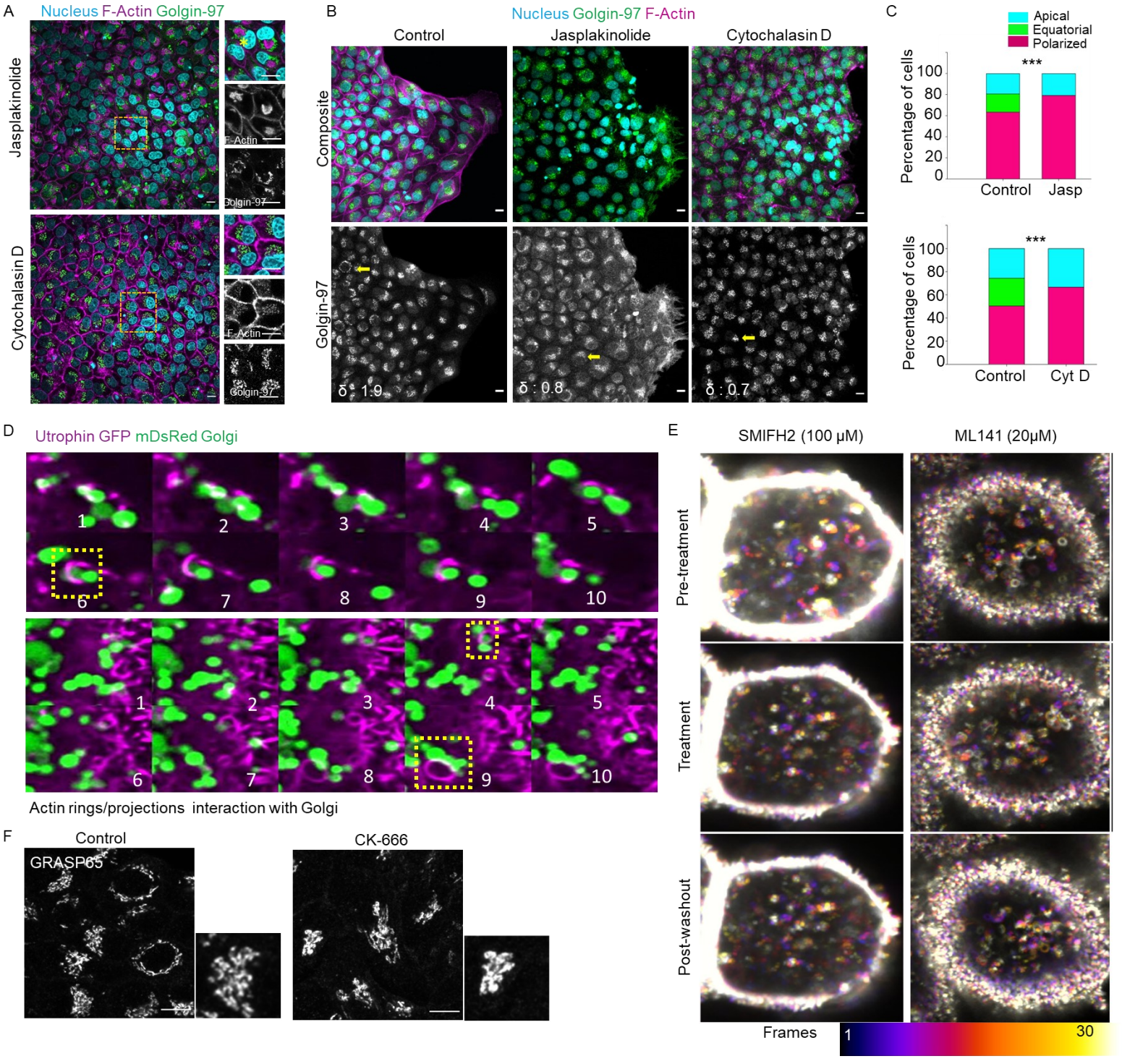

Supplementary Figure 5 : Role of actin dynamics in MIGAR.

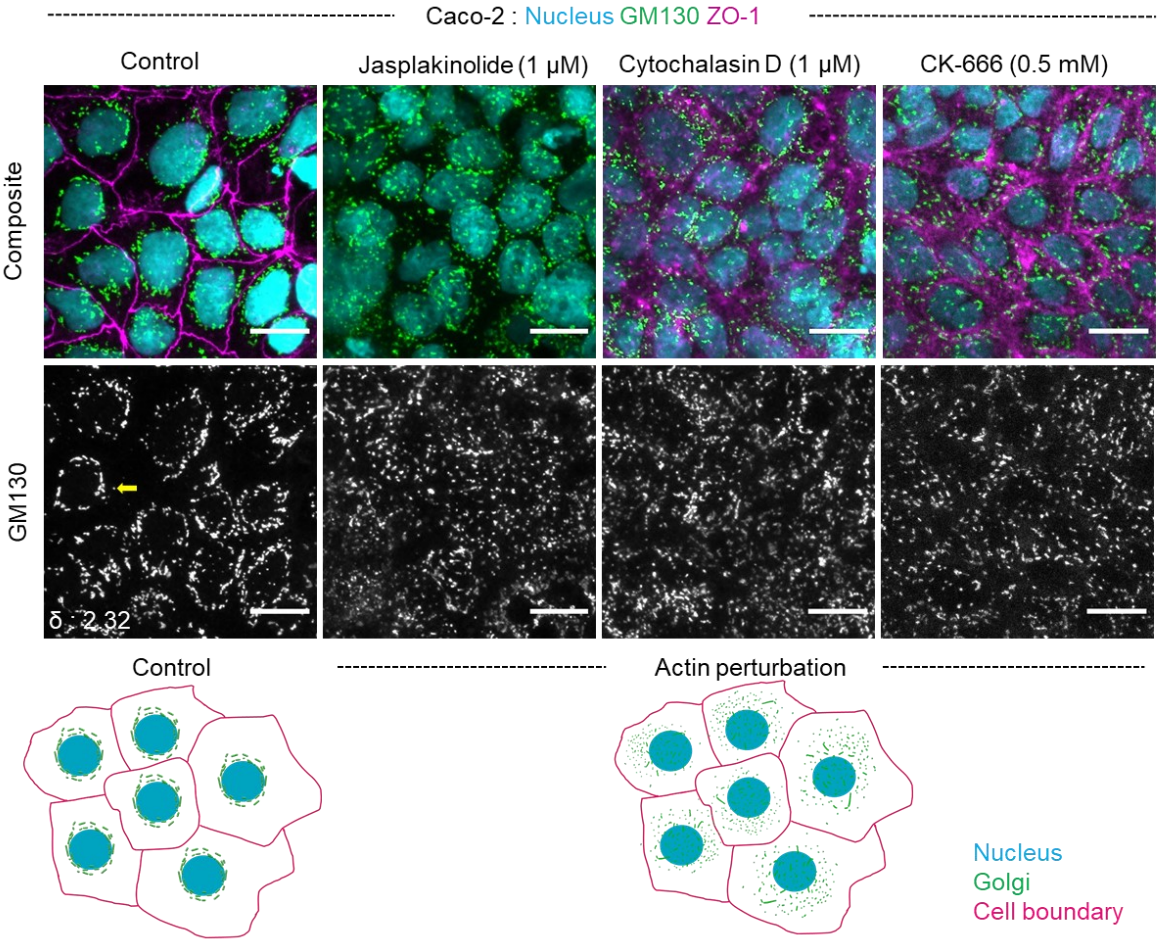

Supplementary Figure 6 : Effect of actin perturbation on MIGAR in Caco-2 cells.

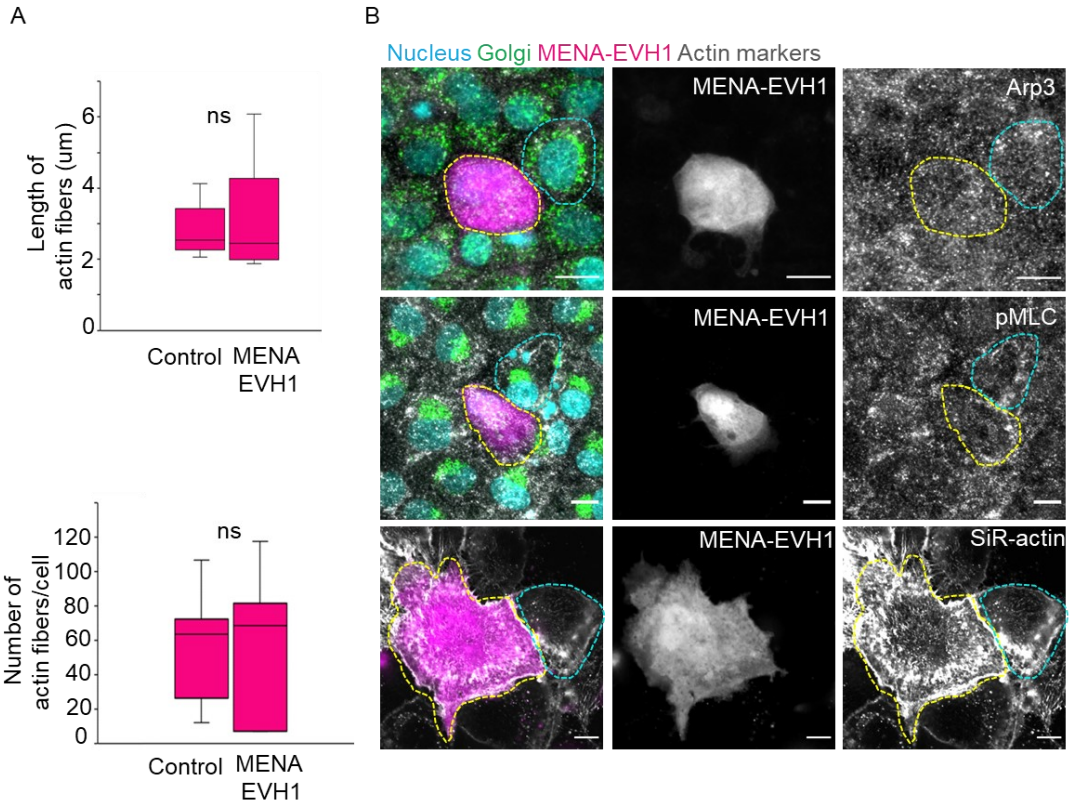

Supplementary Figure 7 : Effect of MENA-EVH1 overexpression on front-rear actin organization.

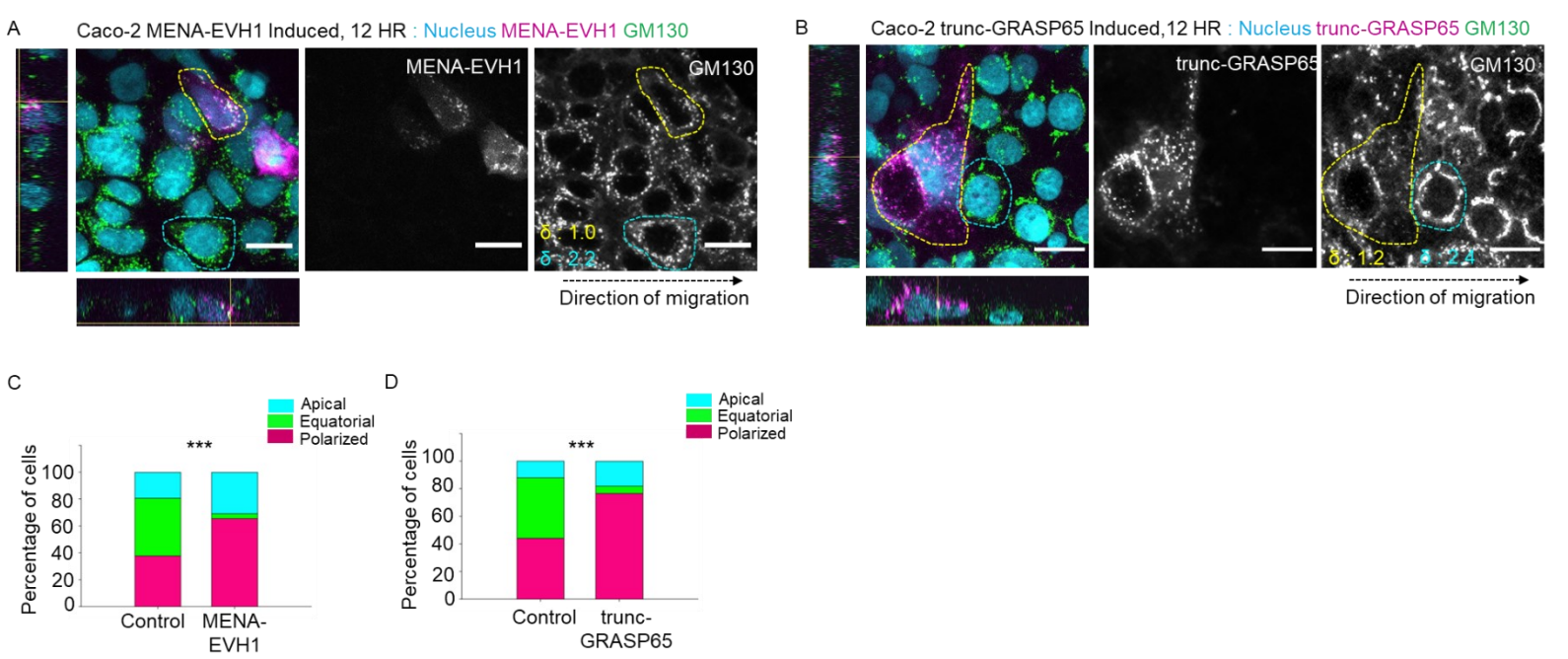

Supplementary Figure 8 : Role of MENA-GRASP65 molecular pathway in MIGAR in Caco-2 collective cell migration.

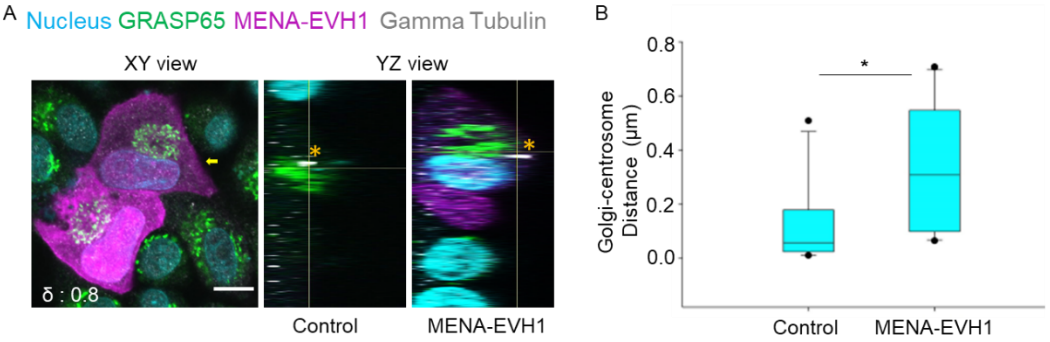

Supplementary Figure 9 : Loss of coherent intracellular polarization under conditions MENA-EVH1 overexpression.

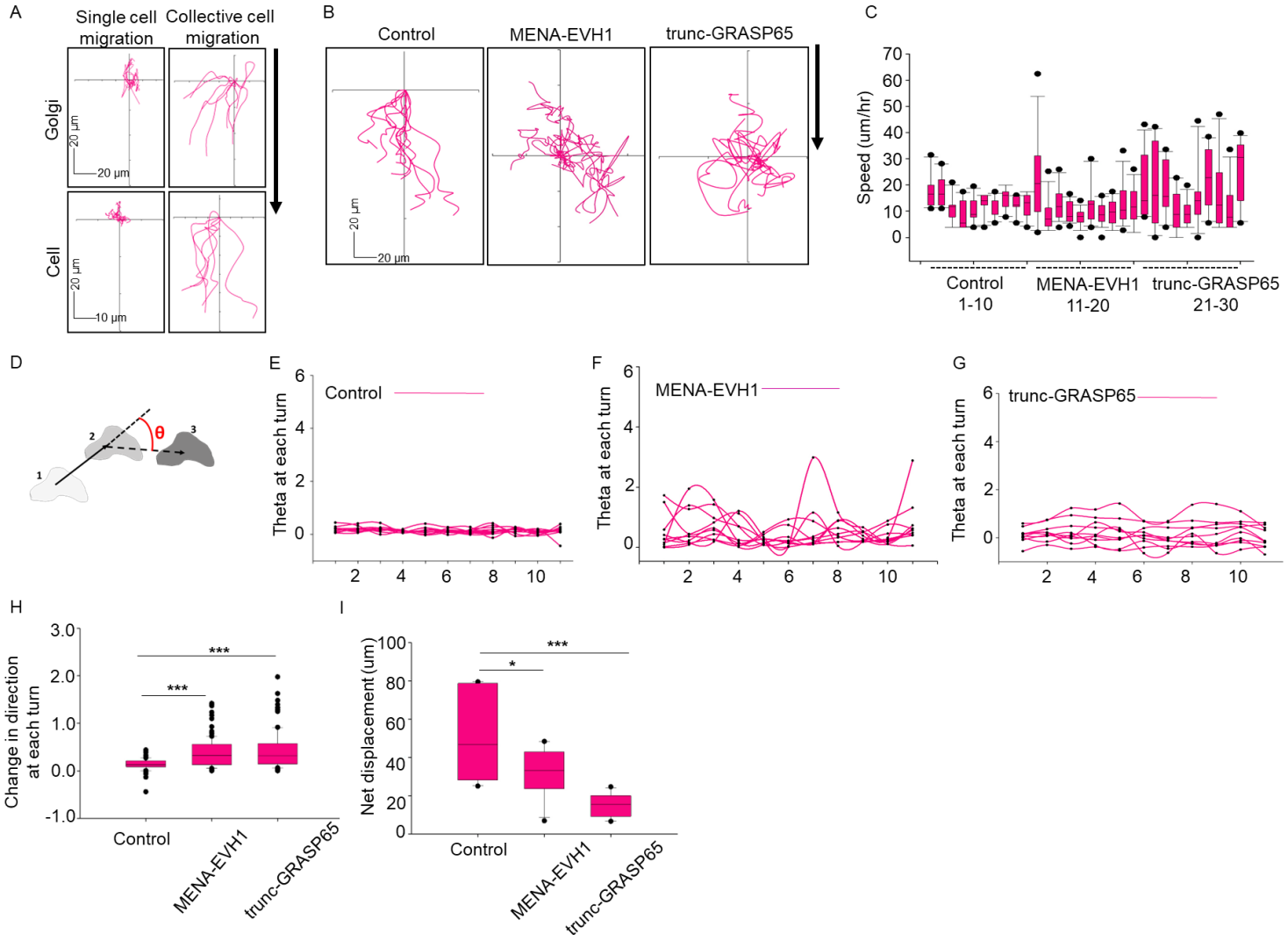

Supplementary Figure 10 : MIGAR is required for coherent intracellular polarization to allow persistent cell migration.